Electronic Supplementary Information

Li$_4$Na$_2$CsB$_7$O$_{14}$: a new edge-sharing [BO$_4$]$^{5-}$ tetrahedra containing borate with high anisotropic thermal expansion

Miriding Mutailipu,[ab#] Min Zhang,[a#] Hao Li,[ab] Xiao Fan,[cb] Zhihua Yang,[a] Gang Wang,[c]* Shifeng Jin,[c] and Shilie Pan[a]*

[a]CAS Key Laboratory of Functional Materials and Devices for Special Environments; Xinjiang Technical Institute of Physics & Chemistry, CAS; Xinjiang Key Laboratory of Electronic Information Materials and Devices, 40-1 South Beijing Road, Urumqi 830011,China

[b]University of Chinese Academy of Sciences, Beijing 100049, China

[c]Research and Development Center for Functional Crystals, Beijing National Laboratory for Condensed Matter Physics, Institute of Physics, Chinese Academy of Sciences, Beijing 100190, China

[#] These authors contributed equally.
*Corresponding authors, E-mails: gangwang@iphy.ac.cn; slpan@ms.xjb.ac.cn

Experimental Section

1. Raw materials

All the raw materials including Li_2CO_3 (LiF) (99.9%), Na_2CO_3 (99.99%), Cs_2CO_3 (CsF) (99%), and B_2O_3 (99.99), were purchased from Aladdin and used as Li, Na, Cs, and B-based precursors for the targeted $Li_4Na_2CsB_7O_{14}$ phase.

2. The single crystal growth and solid-state synthesis of $Li_4Na_2CsB_7O_{14}$

Single crystals of $Li_4Na_2CsB_7O_{14}$ were grown by the high-temperature solution method using LiF-CsF as the flux system in an open atmosphere. A mixture of LiF (0.1038 g, 4 mmol), Na_2CO_3 (0.1060 g, 1 mmol), CsF (0.1519 g, 1 mmol), and B_2O_3 (0.2785 g, 4 mmol) were mixed in an agate mortar, and then moved to a platinum crucible, which were placed in a homemade furnace. The samples were heated at the rate of 100 °C/hour from the room temperature to 630 °C, held for 24 hours, then cooled to 530°C at a rate of 0.5 °C/hour, and then slowly cooled to the room temperature at a rate of 15 °C/hour. Small single crystals were found in the platinum crucible after growth and several single crystals were picked up for further single-crystal X-ray diffraction measurements.

Polycrystalline sample of title compound was synthesized using the solid-state reaction method by mixing Li_2CO_3, Na_2CO_3, Cs_2CO_3, and B_2O_3 according to the stoichiometric ratio. The mixture was preheated at 500 °C for 72 hours. After that, the temperature was gradually raised to 620 °C with several intermediate grindings and mixings, and then held at a certain temperature for 120 hours. Powder X-ray diffraction (PXRD) data were collected using a Bruker D2 PHASER diffractometer at room temperature, with the 2θ ranging from 5 to 70°. The PXRD pattern of polycrystalline sample shows good agreements with the calculated ones (Figure S1). The PXRD data under 300, 400, 500, 600, 700, 800, and 850 K were collected on a Rigaku SmartLab SE powder diffractometer with Cu-Kα radiation and further indexed by Dicvol06.

3. Structure determination

The colorless $Li_4Na_2CsB_7O_{14}$ single crystal with dimensions about $0.11 \times 0.10 \times 0.08$ mm^3 was selected for single-crystal X-ray diffraction. Single-crystal X-ray

diffraction data were collected at room temperature using an APEX II CCD diffractometer using monochromatic Mo Kα radiation and integrated with the SAINT program.[1] The crystal structure was determined through the direct methods and refined by full-matrix least-squares fitting on F^2 using SHELXL.[2] The program PLATON was used for verifying possible missing symmetry elements,[3] but no higher symmetries were found. Crystal data and details of the crystal parameters, data collection, and refinement are listed in Table S1. The atomic coordinates equivalent isotropic displacement parameters, bond valence sum, and selected bond lengths are summarized in Tables S2-S4, respectively.

4. Thermal behavior analysis

Thermal gravimetric analysis and differential scanning calorimetry of $Li_4Na_2CsB_7O_{14}$ were investigated using a NETZSCH STA 449C simultaneous thermal analyzer. The samples and reference Al_2O_3 were placed in a platinum crucible and heated from 40 to 800°C at a rate of 5 °C/min, then cooled to 200°C at a rate of 5 °C/min under flowing nitrogen.

5. Calculation methods

Theoretical calculations including electronic structure and refractive index were based on the methods of density functional theory.[4] The calculations employ the plane-wave pseudopotential method of the CASTEP module.[5] The optimized normconserving pseudopotential[6] in Kleiman-Bylander form for Li $2s^1$, Na $2s^2\,2p^6\,3s^1$, Cs $5s^2\,5p^6\,6s^1$, B $2s^2\,2p^1$, and O $2s^2\,2p^4$ allows us to use a small plane basis set without compromising the accuracy required by the calculation. The exchange correlation interaction was treated by the Generalized Gradient Approximation with the Perdew-Burke-Ernzerhof functional.[7] A kinetic energy cutoff of 830 eV and a Monkhorst-Pack k-point mesh with a density of $2 \times 2 \times 1$ points in the Brillouin zone were chosen for the unit cell. The convergence tests show that these calculation parameters are adequate for this study.

Table S1. Crystal data and structure refinements of $Li_4Na_2CsB_7O_{14}$.

Empirical formula	$Li_4Na_2CsB_7O_{14}$
Formula weight	506.32
Wavelength (Å)	0.71073
Temperature (K)	296(2)
Crystal system	Triclinic
Space group	$P\bar{1}$
a (Å)	6.9395(1)
b (Å)	8.842(2)
c (Å)	10.522(3)
α (°)	95.774(3)
β (°)	105.704(2)
γ (°)	97.395(3)
Z	2
Volume ($Å^3$)	610.1(3)
Density (calc.) (g/cm^3)	2.756
Absorption coefficient (mm^{-1})	3.187
$F(000)$	472
Crystal size (mm^3)	0.11×0.10×0.08
Theta range for data collection	2.35 to 27.53
Limiting indices	$-9 \leq h \leq 8, -8 \leq k \leq 11, -13 \leq l \leq 13$
Reflections collected / unique	3767 / 2708 [R(int) = 0.0167]
Completeness to θ=27.53	98.0%
Data / restraints / parameters	2708 / 0 / 253
Goodness-of-fit on F^2	1.026
Final R indices [I>2sigma(I)][a]	$R_1 = 0.0332, wR_2 = 0.0770$
R indices (all data)[a]	$R_1 = 0.0375, wR_2 = 0.0795$
Largest diff. peak and hole ($e/Å^3$)	1.642 and -1.405

$^aR_1=\Sigma||F_\text{o}| - |F_\text{c}||/\Sigma|F_\text{o}|$ and $wR_2 = [\Sigma w(F_\text{o}^2 - F_\text{c}^2)^2/ \Sigma wF_\text{o}^4]^{1/2}$ for $F_\text{o}^2 > 2\sigma(F_\text{o}^2)$.

Table S2. Atomic coordinates equivalent isotropic displacement parameters and bond valence sum (BVS) for $Li_4Na_2CsB_7O_{14}$.

Atoms	x	y	z	$U_{eq}(\text{Å}^2)$	BVS
Cs(1)	0.9441(1)	0.9485(1)	0.2222(1)	0.030(1)	0.871
Na(1)	0.8190(2)	0.4178(2)	0.1841(2)	0.019(1)	1.116
Na(2)	0.5674(2)	0.5872(2)	0.3348(2)	0.020(1)	1.045
Li(1)	-0.3745(11)	0.1558(9)	-0.0521(8)	0.031(2)	1.121
Li(2)	0.2340(12)	0.6089(10)	0.1257(7)	0.032(2)	0.876
Li(3)	0.4349(10)	0.1437(8)	0.5322(6)	0.018(1)	1.072
Li(4)	0.2567(10)	0.3245(7)	0.3142(6)	0.017(1)	1.035
B(1)	0.4113(6)	0.4019(4)	0.0054(4)	0.009(1)	3.024
B(2)	0.8310(6)	0.3894(5)	0.6169(4)	0.011(1)	2.989
B(3)	1.0315(6)	0.2773(5)	0.4794(4)	0.011(1)	2.986
B(4)	0.835(6)	0.2849(5)	0.0383(4)	0.012(1)	3.035
B(5)	0.4924(6)	-0.0189(5)	0.2742(4)	0.013(1)	3.023
B(6)	0.6531(6)	0.2436(5)	0.3884(4)	0.011(1)	3.066
B(7)	0.4177(5)	0.2044(4)	0.1523(4)	0.010(1)	3.060
O(1)	0.4580(4)	0.0458(3)	0.1566(2)	0.013(1)	2.083
O(2)	0.4610(4)	-0.1698(3)	0.2712(3)	0.019(1)	1.838
O(3)	-0.1161(4)	0.2642(3)	0.0041(3)	0.016(1)	2.107
O(4)	1.0157(4)	0.3481(3)	0.6033(2)	0.017(1)	1.978
O(5)	0.5672(4)	0.0809(3)	0.3948(2)	0.013(1)	2.040
O(6)	0.4793(3)	0.2607(3)	0.0427(2)	0.009(1)	2.148
O(7)	1.2080(4)	0.2460(3)	0.4689(2)	0.015(1)	1.978
O(8)	0.4838(4)	0.4562(3)	-0.1044(2)	0.012(1)	1.982
O(9)	0.1957(3)	0.2038(3)	0.1313(2)	0.013(1)	2.085
O(10)	0.8274(4)	0.4808(3)	0.7244(2)	0.012(1)	1.979
O(11)	0.8581(3)	0.2478(3)	0.3728(2)	0.014(1)	1.994
O(12)	0.1901(4)	0.3881(3)	-0.0200(2)	0.014(1)	2.025
O(13)	0.6577(3)	0.3358(3)	0.5136(2)	0.014(1)	2.000
O(14)	0.5225(3)	0.3029(3)	0.2804(2)	0.010(1)	2.082

Table S3. Anisotropic displacement parameters (Å^2) for Li$_4$Na$_2$CsB$_7$O$_{14}$.

Atom	U_{11}	U_{22}	U_{33}	U_{23}	U_{13}	U_{12}
Cs(1)	0.034(1)	0.022(1)	0.037(1)	-0.005(1)	0.020(1)	-0.001(1)
Na(1)	0.015(1)	0.024(1)	0.016(1)	0.001(1)	0.003(1)	0.005(1)
Na(2)	0.022(1)	0.020(1)	0.016(1)	-0.003(1)	0.003(1)	0.003(1)
Li(1)	0.019(3)	0.028(4)	0.041(4)	-0.020(3)	0.012(3)	-0.003(3)
Li(2)	0.039(4)	0.050(5)	0.023(4)	0.025(4)	0.019(3)	0.032(4)
Li(3)	0.023(3)	0.023(3)	0.011(3)	0.005(2)	0.008(2)	0.007(3)
Li(4)	0.023(3)	0.013(3)	0.018(3)	0.004(2)	0.012(2)	0.005(2)
B(1)	0.012(2)	0.008(2)	0.008(2)	0.001(1)	0.004(1)	0.000(1)
B(2)	0.012(2)	0.010(2)	0.011(2)	0.004(1)	0.005(1)	0.004(1)
B(3)	0.011(2)	0.013(2)	0.010(2)	0.005(1)	0.003(1)	0.003(1)
B(4)	0.012(2)	0.011(2)	0.012(2)	-0.003(1)	0.005(1)	0.001(1)
B(5)	0.013(2)	0.015(2)	0.011(2)	0.003(2)	0.004(1)	0.005(2)
B(6)	0.012(2)	0.013(2)	0.009(2)	0.000(1)	0.002(1)	0.003(1)
B(7)	0.010(2)	0.011(2)	0.009(2)	0.002(1)	0.004(1)	0.001(1)
O(1)	0.023(1)	0.009(1)	0.007(1)	0.001(1)	0.003(1)	0.005(1)
O(2)	0.031(2)	0.012(1)	0.013(1)	0.002(1)	0.004(1)	0.002(1)
O(3)	0.010(1)	0.019(1)	0.017(1)	0.001(1)	0.003(1)	0.003(1)
O(4)	0.012(1)	0.026(2)	0.010(1)	-0.003(1)	0.002(1)	0.004(1)
O(5)	0.017(1)	0.014(1)	0.008(1)	0.002(1)	0.002(1)	0.000(1)
O(6)	0.011(1)	0.007(1)	0.009(1)	0.003(1)	0.005(1)	0.002(1)
O(7)	0.013(1)	0.020(1)	0.014(1)	0.005(1)	0.005(1)	0.006(1)
O(8)	0.017(1)	0.008(1)	0.010(1)	0.002(1)	0.004(1)	-0.001(1)
O(9)	0.010(1)	0.017(1)	0.011(1)	0.004(1)	0.003(1)	0.001(1)
O(10)	0.016(1)	0.012(1)	0.010(1)	0.001(1)	0.004(1)	0.004(1)
O(11)	0.009(1)	0.022(1)	0.011(1)	0.001(1)	0.003(1)	0.004(1)
O(12)	0.011(1)	0.016(1)	0.017(1)	0.007(1)	0.003(1)	0.004(1)
O(13)	0.010(1)	0.020(1)	0.010(1)	-0.002(1)	0.002(1)	0.003(1)
O(14)	0.012(1)	0.010(1)	0.008(1)	-0.001(1)	0.000(1)	0.002(1)

Table S4. The infrared (IR) spectra and calculated vibrational modes of $Li_4Na_2CsB_7O_{14}$.

Experimental IR wavenumber (cm^{-1})	Theoretical IR wavenumber (cm^{-1})
1445	1442
1395	1395
1287	1277
1214	1203
1187	1179
1124	1107
1061	1044
1016	997
927	903
892	875
790	773
727	723
681	676
619	619
500	528
449	438

Table S5. The variation of lattice constants versus temperatures for $Li_4Na_2CsB_7O_{14}$.

Temperature (K)	a (Å)	b (Å)	c (Å)	α (°)	β (°)	γ (°)	V (Å³)
300	6.950	8.844	10.526	95.81	105.41	97.423	612.2518
400	6.9546	8.8741	10.557	95.78	105.70	97.37	615.7553
500	6.960	8.893	10.571	95.77	105.91	97.37	617.6842
600	6.969	8.908	10.607	95.75	105.84	97.34	621.0596
700	6.974	8.916	10.620	95.57	105.87	97.39	623.8260
800	6.976	8.941	10.641	95.65	105.96	97.50	626.3479
850	6.991	8.942	10.646	95.53	105.97	97.529	628.1661

Table S6. The expansivity, estimated standard deviation from room temperature to 850 K for $Li_4Na_2CsB_7O_{14}$ and the components of principal axes relative to the crystallographic axes.

Axes	$\alpha(MK^{-1})$	$\sigma\alpha$ (MK^{-1})	*a*	*b*	*c*
X1	3.5181	2.4716	0.9231	0.0150	0.3843
X2	17.0045	1.9359	0.2221	0.9736	0.0534
X3	25.3882	1.2023	0.5306	-0.1004	-0.8417
V	46.5986	0.9670			

Figure S1. The experimental and calculated XRD patterns of $Li_4Na_2CsB_7O_{14}$.
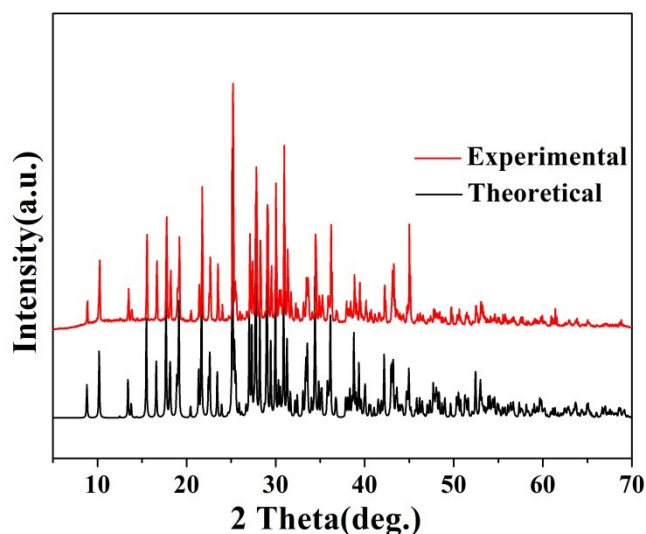
Single crystals of $Li_4Na_2CsB_7O_{14}$ were obtained by high-temperature solution method using a LiF-CsF flux in an open system. The crystal structure was solved and refined based on the collected single crystal X-ray diffraction data, which confirms the existence of edge-sharing $[BO_4]^{5-}$ tetrahedra. Polycrystalline sample of $Li_4Na_2CsB_7O_{14}$ was obtained by solid-state reaction (Figure S1) in an open air and it is stable up to 638 °C without any weight loss, while there is only one obvious peak around 638 and 503 °C on the heating and cooling curves, respectively (Figure S2). Melting experiments demonstrate the incongruently melt behavior of $Li_4Na_2CsB_7O_{14}$, that is why the flux is needed for the crystal growth.

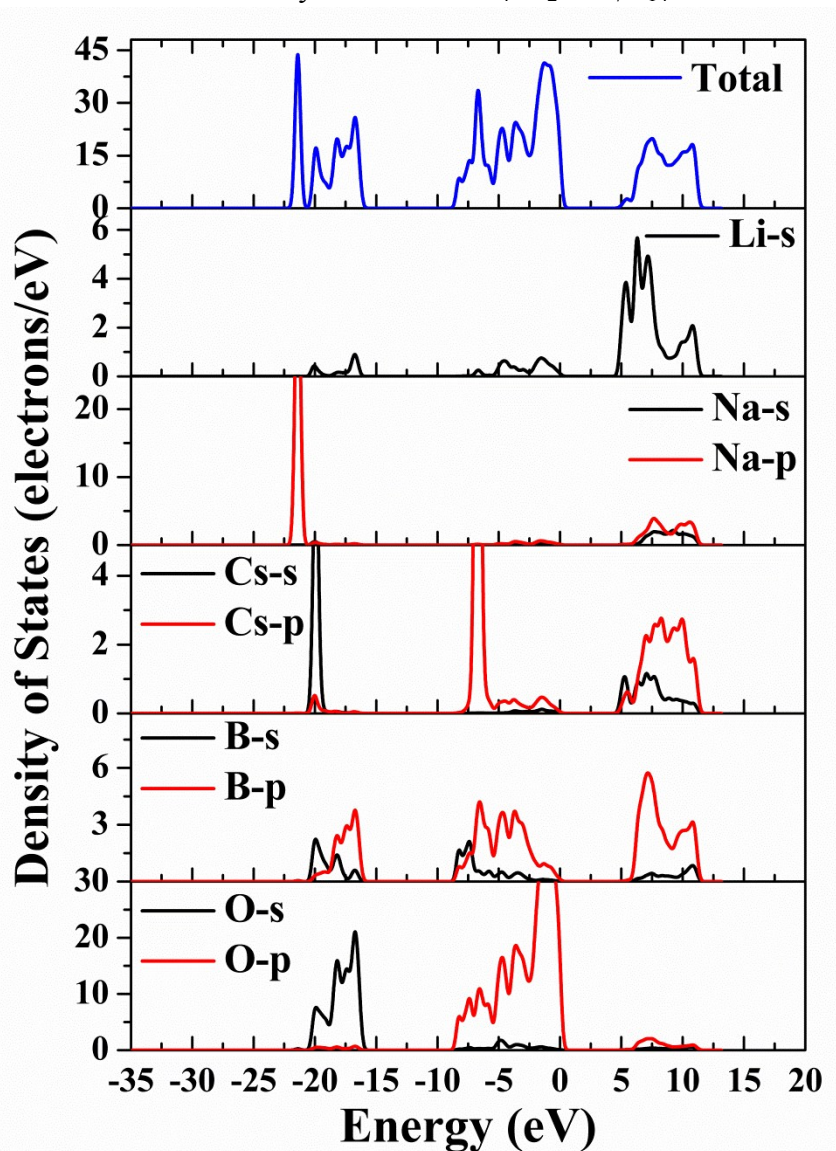**Figure S2.** Thermal gravimetric analysis and differential scanning calorimetry curves of $Li_4Na_2CsB_7O_{14}$.
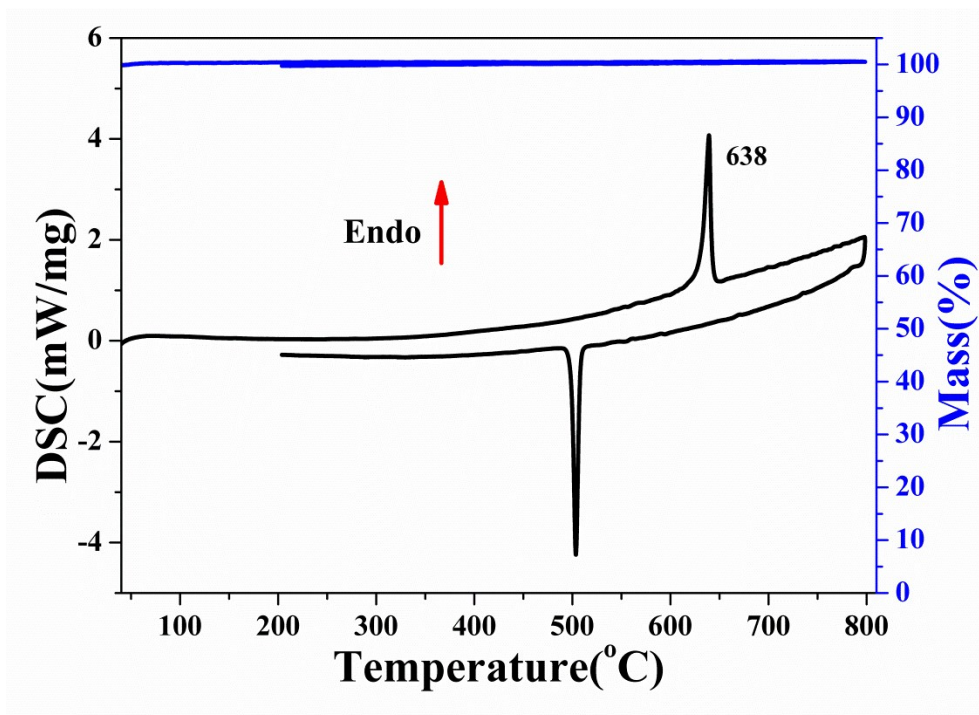
Figure S3. Electronic band structure of $Li_4Na_2CsB_7O_{14}$.

$E_g=4.92 \text{ eV}$
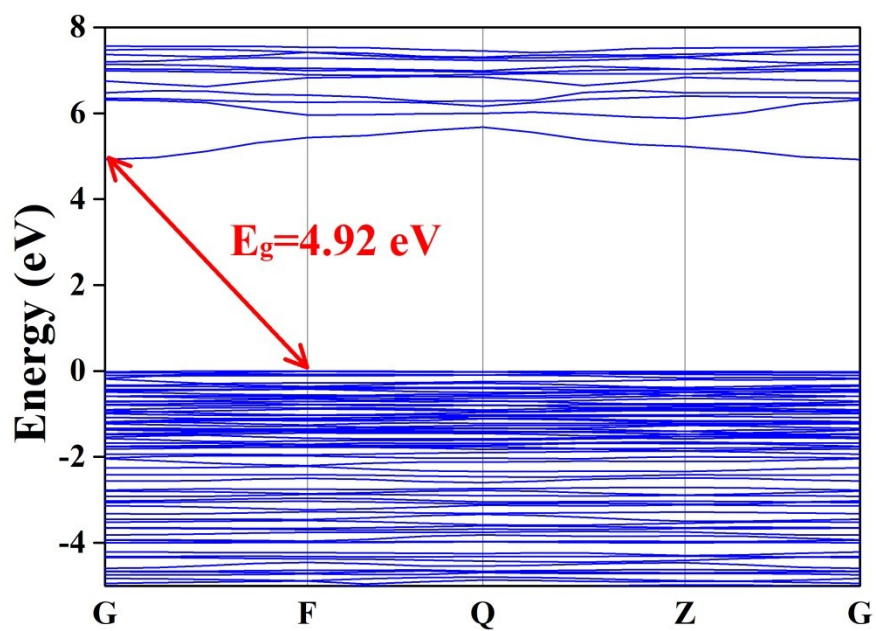
Figure S4. Partial and total density of states of $Li_4Na_2CsB_7O_{14}$.

The electronic band structure and density of states show that $Li_4Na_2CsB_7O_{14}$ has an indirect band gap of 4.93 eV obtained by GGA+PBE (Figure S3). The uppermost part of valence bands from -10 to 0 eV is essentially dominated by O $2p$ states and an appreciable contribution from Cs $2p$ and B $2p$ orbitals with a small amount of Li $2s$ states (Figure S4). The parts from -21.8 to -16.4 eV are mainly generated from O $2s$, B $2s$, and B $2p$, indicating strong sp hybridization of B and O orbitals in the $[B_{14}O_{28}]^{14-}$ basic blocks. While for the bottom of conduction band, it is composed of B $2p$ and M $2p$ (M = Li, Na, and Cs) orbitals. When taking together, we can conclude that the M-O and B-O interactions play a decisive role in determining the band gap of $Li_4Na_2CsB_7O_{14}$.

Figure S5. The highest occupied molecular orbital (a) and the lowest unoccupied molecular orbital (b) of edge-sharing $[BO_4]^{5-}$ tetrahedra in $Li_4Na_2CsB_7O_{14}$.
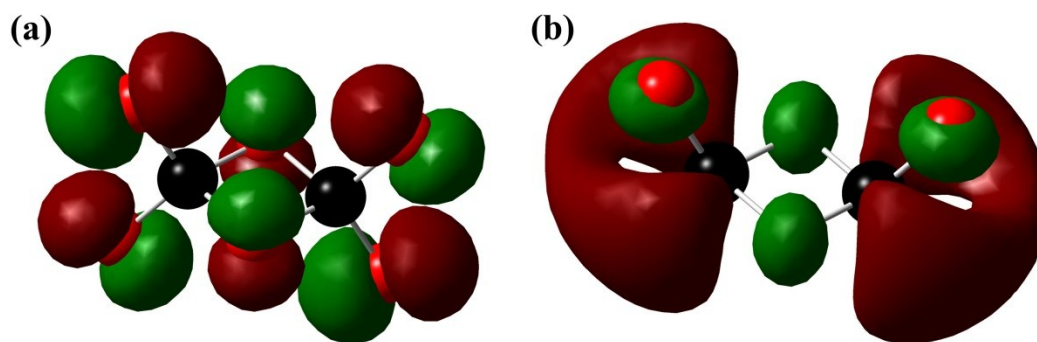
Structure description

While the monovalent cations are 4, 5, 8, 14-coordinated into $Li(1,2,4)O_4$, $Li(3)O_5$, NaO_8, and CsO_{14} polyhedra to fill in the interstitial space and the important roles of these cations can be understood form the following aspects: (1) Those alkali metals free of $d-d$ or $f-f$ electronic transitions, which is beneficial for good transparency in the UV spectral region. (2) The large size atom (Cs) tends to make the whole construction with channels. (3) The chemical bonds of M-O (M = Li, Na and Cs) are typically electrovalent bonds, which can regulate the crystal structure.

References

1. SAINT, *Version 7.60A,Bruker Analytical X-ray Instruments, Inc.,Madison, WI,* 2008.
2. Sheldrick, G. M. *SHELXTL, version 6.12; Bruker Analytical X-ray Instruments, Inc.: Madison, WI,* 2001.
3. Spek, A. L.; *J. Appl. Crystallogr.* 2003, **36**, 7.
4. Rappe, A. M.; Rabe, K. M.; Kaxiras, E.; Joannopoulos, J. D. *Phys. Rev. B* 1990, **41**, 1227.
5. Lin, J. S.; Qteish, A.; Payne, M. C.; Heine, V. *Phys. Rev. B* 1993, **47**, 4174.
6. Lee, M. H. PhD. Thesis, The University of Cambridge 1996.
7. (a) Perdew, J. P.; Burke, K.; Ernzerhof, M. *Phys. Rev. Lett.* 1996, **77**, 3865; (b) Clark, S. J.; Segall, M. D.; Pickard, C. J.; Hasnip, P. J.; Probert, M. J.; Refson, K.; Payne, M. C. *Z. Kristallogr.* 2005, **220**, 567; (c) Heyd, J.; Scuseria, G. E.; Ernzerhof, M. *J. Chem. Phys.* 2003, **118**, 8207; (d) Krukau, A. V.; Vydrov, O. A.; Izmaylov, A. F.; Scuseria, G. E. *J. Chem. Phys.* 2006, **125**, 224106.